RECOVERY OF TARGET IN THE DEEP REGION USING DEPTH–ADAPTIVE VOXEL SIZE RECONSTRUCTION IN DIFFUSE REFLECTIVE OPTICAL TOMOGRAPHY

R. Endoh, M. Fujii and K. Nkayama

Department of Electrical & Electronics Engineering, Sophia University, Tokyo, Japan

endou@kiyoshi.ee.sophia.ac.jp

Abstract: We study diffuse reflective optical tomography using two–dimensional continuous–wave (CW) source–detector arrays on a surface of a semi–infinite medium, aiming at imaging the perfusion and hemoglobin oxygen saturation variation in the human cerebral cortex with brain activation. We formulated the inverse problem with the simple regularized Moore–Penrose inversion [4]. When we uniformly divide a reconstructed region, the reconstruction sensitivity decreases markedly with the depth. Thus, the signal in the deep range may be masked by the unwanted signal in the shallow range. In this report, we propose a depth-adaptive voxel size scheme, in which we assign a larger voxel size to a greater depth. We achieved the recovery of the wanted target using the proposed scheme.

Introduction

Real–time imaging systems [1,5] of the perfusion and hemoglobin oxygen saturation variation in the cerebral cortex using near–infrared light have received in creasing attention because these systems enable non-invasive and non–ionizing measurement of human brain activity. These systems, however, only provide a two-dimensional topogram and cannot discriminate the skin circulation and target organ blood volume. We studied diffuse reflective optical tomography (DROT) using a two–dimensional CW source–detector array, which has depth resolution [3,4]. We formulated the CT algorithm as a simple regularized Moore–Penrose inversion of the forward Rytov approximation for a small perturbation in the absorption change.

One of the difficulties of this type of tomography arises from the strong spatial non–uniformity of the measurement data sensitivity. In other words, since the source–detector arrays are on the surface, the measured data have a much larger sensitivity to the inhomogeneity in the shallow region than to that in the deeper region. Consequently, since the Moore-Penrose inverse seeks the minimum-norm solution, the large data sensitivity in the shallow region is reflected on the large sensitivity of the reconstruction of the inhomogeneity in this region. Thus, in the inversion studied so far, the inhomogeneity signal in the shallow region tends to mask that in the deeper region. This tendency should be mitigated because we are interested in the brain activity rather than the skin circulation. In this article, we divided the shallower region into smaller lateral voxels, that is, depth-adaptive voxel sizes, and demonstrated the ability of the proposed system to discern the wanted signal in the deeper region.

Depth-adaptive voxel size scheme

All the simulations were based on the diffusion equation approximation with an extrapolated zero-boundary condition [2]. The measurement data **y** is assumed as

$$\mathbf{A} \bullet \mathbf{x} = \mathbf{y}, \qquad (1)$$

where **x** is the absorption coefficient change of voxels, and the element of matrix **A** is the measurement signal sensitivity; this is, in practice, calculated using the Rytov approximation. The inverse problem is formulated by the simple regularized inversion [6] of eq. (1) as follows:

$$\mathbf{x} = \mathbf{A}^T \bullet (\mathbf{A} \bullet \mathbf{A}^T + \lambda \mathbf{I})^{-1} \bullet \mathbf{y}, \qquad (2)$$

where **I** is the identity matrix and λ is the Tikhonov regularization parameter [6]. The element of matrix **A** is the measurement data sensitivity of the relative absorption coefficient change at a specific voxel position, which is naturally proportional to the preassigned voxel size. When the number of unknowns is much larger than the number of equations or measurements, such as in the present case, the Moore–Penrose inversion gives the minimum-norm solution. In other words, large elements of matrix **A** for an unknown tend to result in a large value of the inverse solution for that unknown. When we discretize the region of interest into uniform-sized voxels, unknowns in the shallow region have a larger sensitivity in the measurement; thus, the relevant elements in matrix **A** have larger values than those of the deeper region. In order to compensate for these effects, in the depth–adaptive voxel size scheme, we assigned a smaller voxel size in the shallow range so that a resultant element of **A** becomes smaller. In practice, the lateral width of the voxel at each depth is determined so that the maximum elements relevant to each depth in matrix **A** are nearly equal, irrespective of the depth.

Simulation & Results

We assumed a semi-infinite turbid medium at $z \geq 0$. The 4×4 CW source matrix spans $-15 \leq x,y \leq 15$ mm

ISSN: 1727-1983

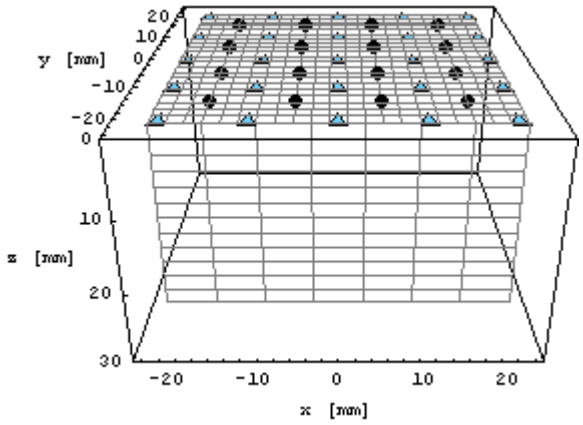

(a) Using uniform voxel size

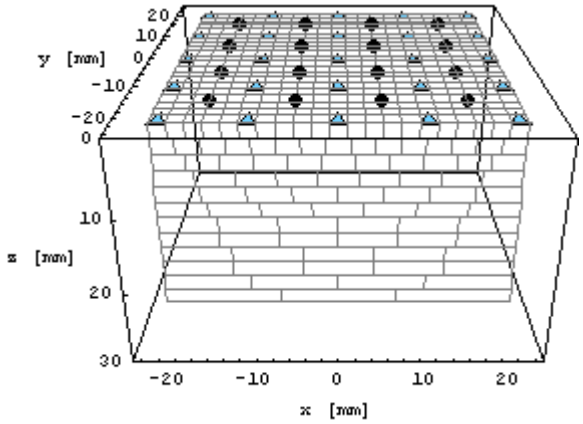

(b) Using depth–adaptive voxel size

Figure 1 Reconstruction models; model a) is uniformly divided into 7 × 7 × 12 voxels and model b) is divided into 1128 depth-adaptive sized voxels. Circles denote source positions. Triangles denote detector positions.

and the 5 × 5 detector matrix spans –20 ≤ x,y ≤ 20 mm at the surface z = 0 mm. The region of interest spans –21 ≤ x,y ≤ 21 mm and 0 ≤ z ≤ 16 mm. The turbid medium was assigned with the typical optical properties of μ'_{s0} = 1 mm^{-1} and μ_{a0} = 0.006 mm^{-1}.

Fig. 1 shows the reconstruction models: one is uniformly divided into 7 × 7 × 12 voxels and the other is divided into 1128 depth-adaptive sized voxels. We set the voxel size at the target depth of z = 11 mm for each model to be equal. We estimated of each voxel as well as 5 × 5 source coupling factors and 4 × 4 detector coupling factors as unknowns from the 400 measurement data for both the reconstruction models.

We simultaneously simulated two objects with $\delta\mu_a$ = 0.001 mm^{-1} having dimensions of 6 × 6 × 2 mm; one was centred at (x, y, z) = (–10, 0, 3) mm and the other at (10, 0, 11) mm, possibly representing the skin circulation change and brain activity, respectively. Further, we reconstructed the absorption coefficient

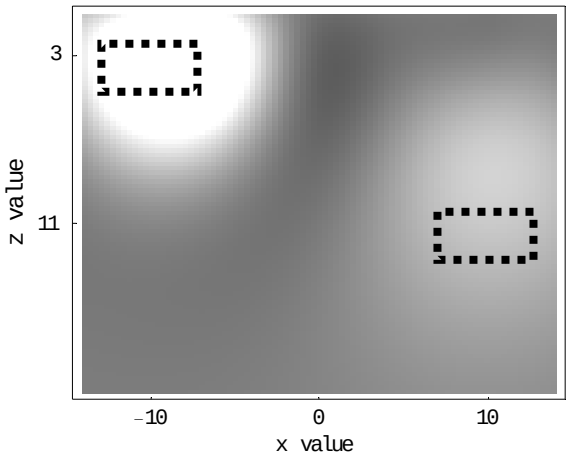

(a) Uniform voxel size scheme

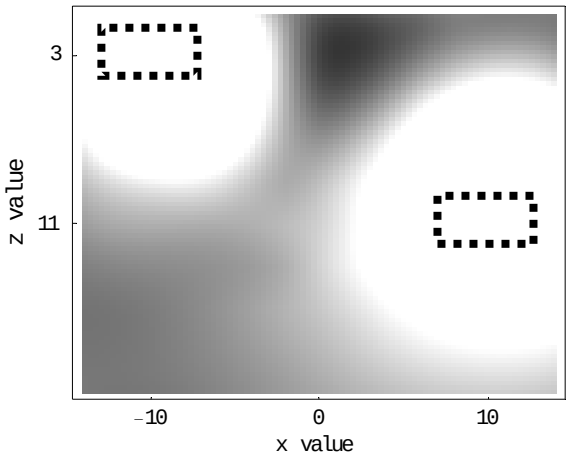

(b) Depth–adaptive voxel size scheme

Figure 2 x–z cross-sectional images at y = 0 mm (measurement $S_{0,max}$ / N = 160 dB). Greyscale is linear and is in the range of -10^{-4} (black) ≤ $\delta\mu_a \leq 10^{-4}$ (white). Dotted rectangles indicate objects.

changes with a regularization parameter of $\lambda = 10^{-3}$. Fig. 2 shows the x–z cross–sectional images, and Fig. 3 shows the x–y plane images at z = 11 mm, where the wanted target should be reconstructed.

Discussion

In Fig. 2(a), the shallow target in the high sensitivity region is reconstruction of the much stronger than that of the deep target in the low sensitivity region, and it may be masked by the shallow unwanted signal. On the other hand, in Fig. 2(b), using the depth–adaptive voxel size scheme, the wanted deep target is reconstructed at the correct position and intensified as compared with that using the uniform voxel size scheme. This clearly demonstrates a improvement in the reconstruction by

ISSN: 1727-1983

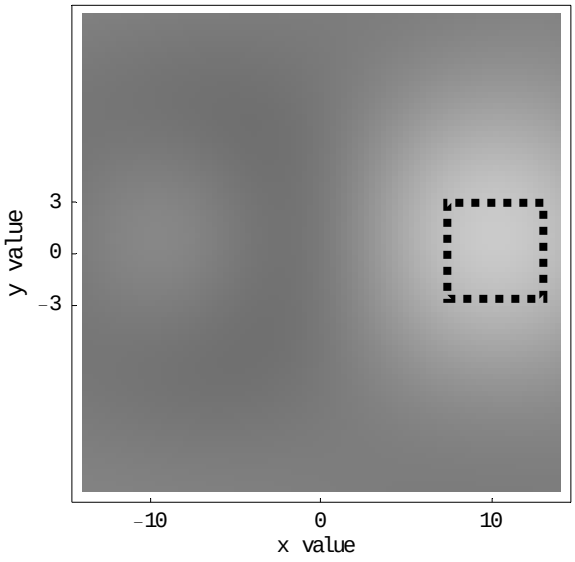

(a) Uniform voxel size scheme

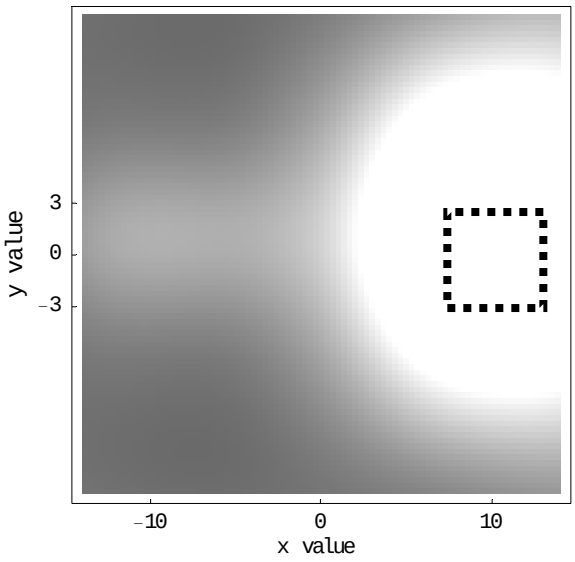

(b) Depth–adaptive voxel size scheme

Figure 3 x–y plane images at z = 11 mm (measurement $S_{0,max}$ / N = 160 dB). Greyscale is linear, is in the range of -10^{-4} (black) ≤ $\delta\mu_a \leq 10^{-4}$ (white). Dotted rectangles indicate objects.

using the proposed scheme.

As evident from Fig. 3(a) by using the uniform voxel size scheme, we cannot see any clear objects. On the other hand, we can clearly see only the wanted signal in Fig. 3(b) by using the depth–adaptive voxel size scheme. This is an important result because in the actual brain activity measurement, the x–y plane images at the cerebral cortex surface would be used for clinical examination.

In the actual measurement, the measurement noise is primarily determined by the shot noise of the detector. If we assume a parallel measurement scheme with all the sources switched on, by using frequency division modulation for the sources, the shot noise is determinded by $S_{0,max}$, which is the baseline detector signal from the nearest source. From this standpoint, we have been using $S_{0,max}$ / N to prescribe the noise condition. Apparently, $S_{0,max}$ / N = 160 dB, which is needed for this particular simulation model, seems unrealisable for the real–time measurement having an appropriate signal band width for the brain circulation change. The wanted $S_{0,max}$ / N value, however, is extremely dependent on the source–detector configurations and the region of interest. Further, if we incorporate the time division scheme in the measurement, the required S_0 / N value will be reduced considerably because we become concerned with the shot noise generated by the baseline signal from the second–nearest or third–nearest sources. All these practical considerations and designs are needed for the actual realization of DROT for brain activity measurement.

Conclusions

We proposed the depth–adaptive voxel size scheme in the inverse problem of continuous–wave DROT using two–dimensionl source–detector arrays on the plane surface of a semi–infinite medium. We simulated two targets, which existed at depths of z = 3 and 11 mm, assuming the skin circulation and blood volume of an adult brain. The reconstructed images clearly show that the reconstructed signal sensitivity in the target region was intensified by using the proposed scheme.

Further study is needed on the practical confinement of the region of interest, corresponding optimal arrangement of source–detector and the data acquisition scheme to realize the actual DROT for brain activity measurement.

Acknowledgement

This work was partially supported by MEXT (or JSPS) KAKENHI 15300169.

References

[1] HITACHI MEDICAL CORPORATION, OPTICAL TOMOGRAPHY SYSTEM, Internet site address: http://www.hitachi-medical.co.jp/opt-e

[2] R. C. HASKELL, L. O. SVASAND, T. TSAY, T. FENG, M. S. MCADAMS and B. J. TROMBERG (1994): 'Boundary conditions for the diffusion equation in radiative transfer', *J. Opt. Soc. Of Am.*, **A11**, pp. 2727-2741

[3] R. ENDOH, A. SUZUKI, M. FUJII, and K. NAKAYAMA (2002): 'Simulation study on diffuse reflective optical tomography', Proc. of Asian Symposium on

ISSN: 1727-1983

Biomedical Optics and Photomedicine, Japan, 2002, pp. 70-61

[4]R. ENDOH, A. SUZUKI, M. FUJII, and K. NAKAYAMA (2004): 'Fundamental study on diffuse reflective optical tomography', *Phys. Med. Bio.*, **49**, pp. 1881-1889

[5]SIMADZU CORPORATION, NIRSTATION, Internet site address:http://www.med.shimadzu.co.jp/products/om/01.html

[6]T. MUSHA and Y. OKAMOTO (1992): 'Inverse problems and their solutions (in Japanese)', (Ohmusha, Tokyo)

ISSN: 1727-1983